J Mater Sci (2007) 42:7337–7342
DOI 10.1007/s10853-007-1576-z

Mechanical properties and electronic structures of compressed C_{60}, C_{180} and $C_{60}@C_{180}$ fullerene molecules

Haijun Shen

Received: 21 December 2006 / Accepted: 31 January 2007 / Published online: 15 May 2007

Abstract Molecular dynamics simulations were performed for compressed C_{60}, C_{180} and $C_{60}@C_{180}$ fullerene molecules, and the semi-empirical PM3 calculations were carried out to obtain the electronic structure of the compressed fullerenes. According to the obtained results, the differences of mechanical properties between these compressed fullerenes, as well as the changes of their FMO (Frontier molecular orbital) energy-levels during compression, were discussed. It is shown that (1) the C_{60} molecule has much higher load-support and energy-absorbing capability than the C_{180} and $C_{60}@C_{180}$ molecules, and the $C_{60}@C_{180}$ is only slightly superior to the C_{180}, (2) of the three molecules, the C_{60} molecule has the best chemical-stability, and the $C_{60}@C_{180}$ molecule has the worst one, (3) with the increase of compressive strain, both the C_{60} and $C_{60}@C_{180}$ molecules become more chemically active, and (4) when the compressed C_{180} molecule caves in at the loading position(s), its chemical-stability decreases abruptly.

Introduction

Since the C_{60} fullerene was first discovered in 1985 [1], some other spherical carbon-molecules, such as C_{24}, C_{36}, C_{70}, C_{80}, C_{180}, C_{240} and so on [2–4], were also obtained during the next decade. Due to their special structure, the carbon fullerene molecules have attracted tremendous attentions from physicists, chemists and material designers. Now many endohedral fullerenes, i.e. the carbon fullerenes encapsulating guest atoms or molecules, have been obtained in laboratory. The endohedral fullerenes include $M@C_{82}$ (M = Hf, Ti, U), $M@C_{60}$ (M = BH_3, CH_4, NH_3), $M@C_{80}$ (M = Be, C, Si, Ge) and so on [5–9]. Interestingly, recently the $C_{60}@C_{180}$ molecule, i.e. the C_{180} encapsulating one C_{60} fullerene, see Fig. 1c, was also reported [10].

Researches show that carbon fullerenes and endohedral fullerenes have particular mechanical and photoelectric properties [11–13], and are applicable to material modification, micro/nano electromechanical systems, quantum devices and so on. However, up to now the mechanical and electronic properties of the compressed $C_{60}@C_{180}$ have not been reported yet as far as we know.

Due to the fact that carbon fullerenes have very small size, it is often very difficult to test their mechanical and electronic properties through STM (Scanning tunnel microscope) or AFM (Atomic force microscope). However, the MD (Molecular dynamics) and QM (quantum mechanics) methods provide convenience for theoretically analyzing the properties of carbon fullerenes, where the MD simulations can be used to reveal the movement details of atoms and the deformation of molecules [14], whereas the QM simulations can give the electronic structure of the deformed molecules.

In the present paper, the radial compression of the $C_{60}@C_{180}$ molecule, as well as its internal and exterior ‘‘cages’’, i.e. the C_{60} and C_{180} molecules, is simulated by the MD method, and the changes of their geometrical configurations, energy and external loading during compression are obtained and analyzed. Then the electronic structure of the compressed fullerenes is calculated by the semi-empirical QM method of PM3 (Parametric Method 3 [15]), and their chemical-stability during compression is

---

H. Shen (✉)
School of Aeronautics & Astronautics, Nanjing University of Aeronautics & Astronautics, Nanjing 210016, China
e-mail: shj@nuaa.edu.cn

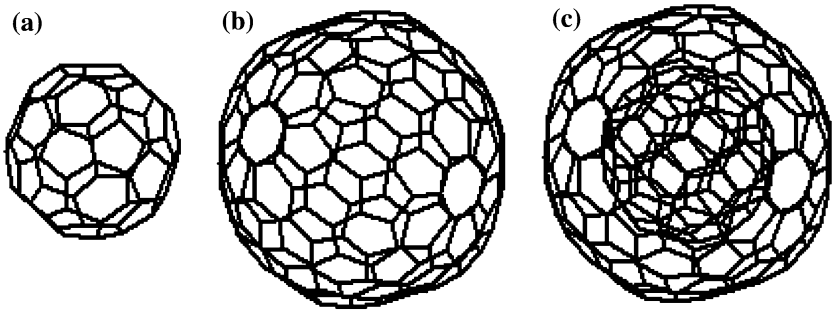

Fig. 1 The (**a**) C_{60}, (**b**) C_{180} and (**c**) $C_{60}@C_{180}$ fullerene molecules

discussed according to the calculated FMO (Frontier molecular orbitals) energy-levels.

The paper reveals the mechanical properties and the electronic structure changes of the C_{60}, C_{180} and $C_{60}@C_{180}$ molecules under compression, and some correlative results are very helpful for researchers to recognize the properties of the cage-like carbon molecules.

Method and model

In this paper the MD method is used to simulate the radial compression of the C_{60}, C_{180} and $C_{60}@C_{180}$ molecules. In MD, the time evolution of interacting atoms is followed by integrating their equations of motion, which can help people to comprehend more details of matter motion at atomic level. Generally speaking, many-body potentials can more accurately describe the interactions between atoms than simple pair-potentials. Of the available many-body potentials, Brenner's REAO (Reactive empirical bond order) potential [16–18], a famous bond order potential derived from quantum-mechanical arguments, can well consider bond order and covalent bonds forming/breaking for the carbon elements and has been widely used to calculate the lattice constants, bulk modulus and cohesive energy of diamond, graphite and carbon nanotubes [16, 17, 19]. In the present paper the REAO potential is used to describe the interactions between the carbon atoms of all the C_{60} and C_{180} ''cages'' (or molecules). The formula and parameters of the REAO potential for carbon systems take the one of Refs. [20] and [21]. For the interaction between the C_{60} and C_{180} cages of the $C_{60}@C_{180}$ molecule, the L-J(12-6) pair-potential [22], i.e., $V(r) = 4\varepsilon[(\sigma/r)^{12} - (\sigma/r)^{6}]$, is taken when $r > 0.18$ nm, and the REAO potential is taken when $r \leq 0.18$ nm. Here r is the distance of carbon atoms, $\varepsilon = 37$ K and $\sigma = 0.3345$ nm.

The following steps are taken to simulate the compression of the C_{60}, C_{180} and $C_{60}@C_{180}$ molecules: (1) adjusting the distance h of two farthest carbon atoms of the fullerenes; (2) ''fixing'' the two atoms, relaxing other carbon atoms through MD method, and obtaining the energy E and external loading F corresponding to the compressive displacement Δh; (3) repeating Steps (1) and (2), and obtaining a series of E and F data corresponding to different Δh. Here compressive strain l is defined as $\Delta h/h_0$, and h_0 is the initial diameter of the fullerene molecules.

In the MD simulations the Varlet's expression of velocity [22], the time-step of 0.001 ps and the temperature of 300 K are taken. The constant temperature is controlled by the Nose technique [23].

Figure 1 presents the investigated C_{60}, C_{180} and$C_{60}@C_{180}$ fullerene molecules. The molecules are geometrically optimized at 300 K by MD method, and their molecular weight, diameter, volume and system energy are listed in Table 1. By comparing the system energy of the C_{60} molecule with the one by the Brenner-potential based MD method in Ref. [24], it is found that the present value of –408.52 eV is very close to the one of Ref. [24], i.e. –408.6 eV, which indirectively validates the present MD method.

Once the geometrical configurations of the compressed fullerene molecules are given through the above MD method, the electronic structure of the compressed fullerene molecules can be obtained by the QM method.

It is very difficult to accurately solve a multi-atomic system and obtain its energy and wave-function by Schrödinger's equation. However, the solution of the Schrödinger's equation for a multi-atomic system can be simplified into one single-electronic problem, i.e. the solution of the Hartree–Fock equation, through the Born–Oppenheimer assumption, by which the motion of electrons and nuclei can be decoupled, the Hartree–Fock assumption and the LCAO (Linear combination of atomic orbitals) assumption [25, 26]. The PM3 is one semi-empirical QM method just based on the above arguments, and it only considers the valence electrons of atoms and ignores the three and four center integral of the Fock matrix in the Hartree–Fock equation [26]. Despite the simplifications, lots of researches show that the PM3 method is still effective in calculating heat-of-formation, geometrical configuration and electronic structure of organic molecules [25].

The PM3 calculations are performed in the quantum-chemical software of Gaussian03®. In the calculations, the

Table 1 Molecular weight, diameter, volume, and energy of the C_{60}, C_{180} and C_{60}@C_{180} molecules

Fullerene molecules	C_{60}	C_{180}	C_{60}@C_{180}
Molecular weight	720	2,130	2,850
Diameter h_0 (nm)	≈0.75	≈1.21	≈1.24
Molecular volume (nm^3)	≈1.22	≈3.20	≈5.86
System energy (eV)	≈–408	≈–1,279	≈–1,695

closed shell model and self-consistent field (SCF) approach are taken. The convergence limit takes 0.042 kJ/mol.

Results and discussions

Compressive properties of C_{60}, C_{180} and C_{60}@C_{180} molecules

Figures 2–4, respectively, present the configuration evolvement of the C_{60}, C_{180} and C_{60}@C_{180} molecules under compression. In these figures the loading positions are marked with arrowheads. From Figs. 2–4, it can be found that during the compression all the C_{60}, C_{180} and C_{60}@C_{180} molecules cave in at the loading position(s), see Figs. 2c, 3b, c and 4b–d, respectively, but their configuration evolvements are still very different. First, the C_{60} molecule has the evolvement mode of ‘‘compressive deformation and simultaneous cave-in at two loading positions’’, but both the C_{180} and C_{60}@C_{180} molecules have the mode of ‘‘compressive deformation, cave-in at one loading position and then at two loading positions’’. Second, due to the support of the internal C_{60}, the depth of the carve-in of the compressed C_{60}@C_{180} molecule is much smaller than that of the C_{180} molecule. Third, when strain l reaches about 41%, see Fig. 4d, the local reconfiguration of atoms occurs to the C_{60}@C_{180} molecule near its loading positions, but the C_{60} and C_{180} molecules have no the reconfiguration phenomenon. Further MD simulations show that when the locally reconfigured C_{60}@C_{180} molecule is unloaded, its configuration cannot be restored, but the compressed C_{60} and C_{180} molecules without local reconfiguration can restore their configurations, which implies that the C_{60}@C_{180} molecule has failed at strain l = 41%. In addition, during the whole compression, the internal C_{60} of the C_{60}@C_{180} molecule is not found to cave in.

Figure 5a and b, respectively, present the changes of ΔE and external loading F of the C_{60}, C_{180} and C_{60}@C_{180} molecules under compression. Here the ΔE is the averaged energy-increment per atom. In Fig. 5b, the arrowheads ‘‘↑’’ and ‘‘↓’’, respectively, mark the moments of the

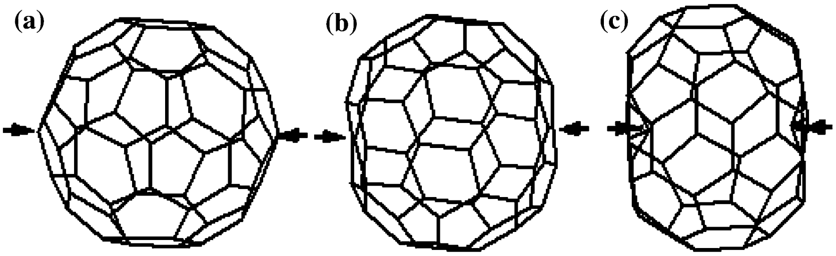

Fig. 2 The compressed C_{60} molecule. (**a**) l = 0%, (**b**) l = 25% and (**c**) l = 41%

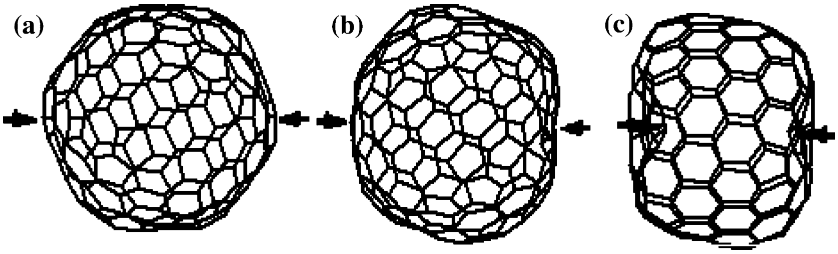

Fig. 3 The compressed C_{180} molecule. (**a**) l = 0%, (**b**) l = 18% and (**c**) l = 52%

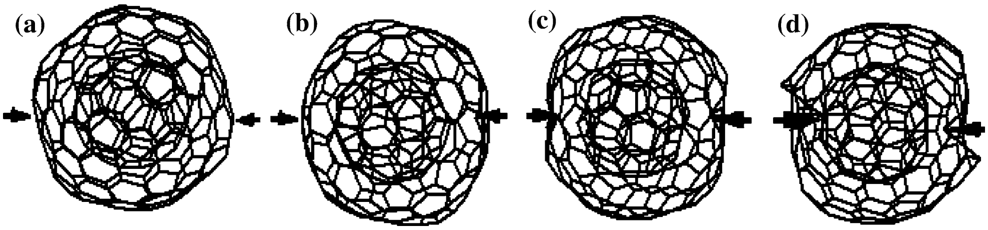

Fig. 4 The compressed C_{60}@C_{180} molecule. (**a**) l = 0%, (**b**) l = 21%, (**c**) l = 36% and (**d**) l = 41%

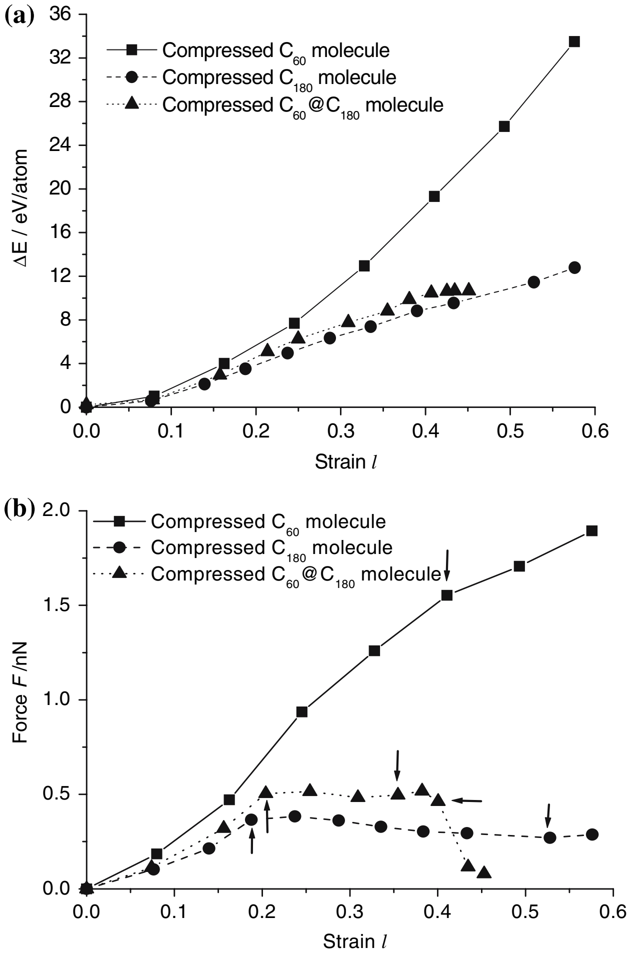

Fig. 5 (**a**) Energy and (**b**) external-loading of the compressed C_{60}, C_{180} and $C_{60}@C_{180}$ molecules

cave-in at one and two loading-position(s) for the compressed C_{60}, C_{180} and $C_{60}@C_{180}$ molecules, and the arrowhead " ← " marks the moments of the $C_{60}@C_{180}$ molecule failing.

According to Fig. 5a, it is found that (1) under same strain l, the ΔE of the C_{60} molecule is much higher than those of the C_{180} and $C_{60}@C_{180}$ molecules, which implies that the C_{60} molecule has higher energy-absorbing capability, (2) the ΔE–l curve of the $C_{60}@C_{180}$ molecule is slightly higher than that of the C_{180} molecule, which implies that the C_{180} and $C_{60}@C_{180}$ molecules have only small difference in energy-absorbing, and (3) the ΔE–l curve of the $C_{60}@C_{180}$ molecule is unequal to not only the average but the addition of the ΔE–l curves of the C_{60} and C_{180} molecules.

According to Fig. 5b, it is found that

(1) For same strain level, the external loading F of the C_{60} is obviously higher than those of the C_{180} and $C_{60}@C_{180}$ molecules, which denotes the C_{60} molecule has best loading-support capability.
(2) With the increase of strain, the external loading F of the compressed C_{60} molecule increases monotonically, but after the C_{60} caving in at the loading positions the increase of the external loading F slows down.
(3) With the increase of strain, the loading F of the C_{180} and $C_{60}@C_{180}$ molecules increases first; when they cave in at one loading position, their loading F decreases and then increases again.
(4) The C_{180} and $C_{60}@C_{180}$ molecules have comparative loading-support capability. The maximal loading of the C_{180} molecule is about 3.83 nN, and the $C_{60}@C_{180}$ molecule about 4.91 nN.
(5) The $C_{60}@C_{180}$ molecule fails at $l \approx 41\%$; after this the external loading F decreases sharply.
(6) The F–l curve of the $C_{60}@C_{180}$ molecule is unequal to not only the average but the addition of the curves of the C_{60} and C_{180} molecules.

Electronic structure of C_{60}, C_{180} and $C_{60}@C_{180}$ under compression

According to the FMO theory [26, 27], it is considered that the FMOs, i.e. the MOs (Molecular orbitals) near the LUMO (Lowest unoccupied molecular orbital) and HOMO (Highest occupied molecular orbital), determine the chemical properties of one molecule. The LUMO and

Fig. 6 The FMO energy-levels of the compressed (**a**) C_{60}, (**b**) C_{180} and (**c**) $C_{60}@C_{180}$ molecules

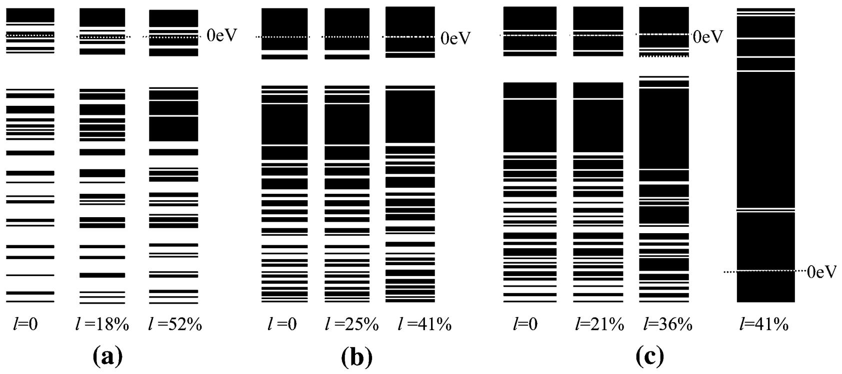

HOMO energy can reflect molecular electrophilicity and nucleophilicity, respectively. The LUMO energy is close to the molecular electrophilic-potential in value, and the higher the HOMO energy is, the easier the molecule loses its electron. The energy-gap between the LUMO and HOMO can reflect the capability of electron transferring from the occupied MO to the unoccupied one. So in the present paper the FMO energy and the LUMO–HOMO energy-gap for the compressed molecules are mainly discussed.

By PM3 calculations, Fig. 6a–c present the changes of the FMO energy-levels for the three molecules during compression. In Fig. 6 the horizontal dashed-lines give the position of 0 eV, the energy range of the last one of Fig. 6c is –5 to 40 eV, and the ranges of the others are –40 to 5 eV. Figure 7a–c present the changes of the HOMO and LUMO energy as well as the LUMO–HOMO energy-gap for the compressed C_{60}, C_{180} and $C_{60}@C_{180}$ molecules.

From Fig. 6 it can be found that due to the configuration change of the compressed fullerenes their MO energy-levels change, and especially after the compressed $C_{60}@C_{180}$ molecule is locally reconfigured at the loading positions, i.e., after $l = 41\%$, its MO energy-levels change sharply, see Fig. 6c.

From Fig. 7 it can be seen that

(1) The LUMO, HOMO energy and the LUMO–HOMO energy-gap for the undeformed C_{60} molecule are –3.18, –9.41 and 6.23 eV, respectively, those of the undeformed C_{180} molecule are –3.74, –8.82 and 5.08 eV, and those of the $C_{60}@C_{180}$ molecule are -3.78, -8.71 and 4.93 eV. Both the LUMO energy and the LUMO-HOMO energy-gap have the order of $C_{60} > C_{180} > C_{60}@C_{180}$, but the HOMO energy has the contrary order of $C_{60} < C_{180} < C_{60}@C_{180}$, which denotes that the $C_{60}@C_{180}$ molecule is easiest to lose electron and has the worst chemical-stability, and the C_{60} molecule has the best one.

(2) For the C_{60} molecule as well as the $C_{60}@C_{180}$ molecule before failure, with the increase of compressive strain their LUMO energy and LUMO–HOMO energy-gap decrease, but their HOMO energy increases, which implies that the compressed C_{60} and $C_{60}@C_{180}$ molecules have lower energy quantum excitation of HOMO electron(s) and become more chemically active.

(3) For the C_{180} molecule, the changes of its HOMO, LUMO energy and LUMO–HOMO energy-gap are different during compression. At the moments of the C_{180} carving in at one and two loading-position(s), both its HOMO energy and LUMO–HOMO energy-gap reach local maximum, but its LUMO energy local minimum, which implies that the compressed C_{180} molecule has lower energy quantum excitation of HOMO electron(s) and becomes more chemically active when it carves in at the loading-position(s).

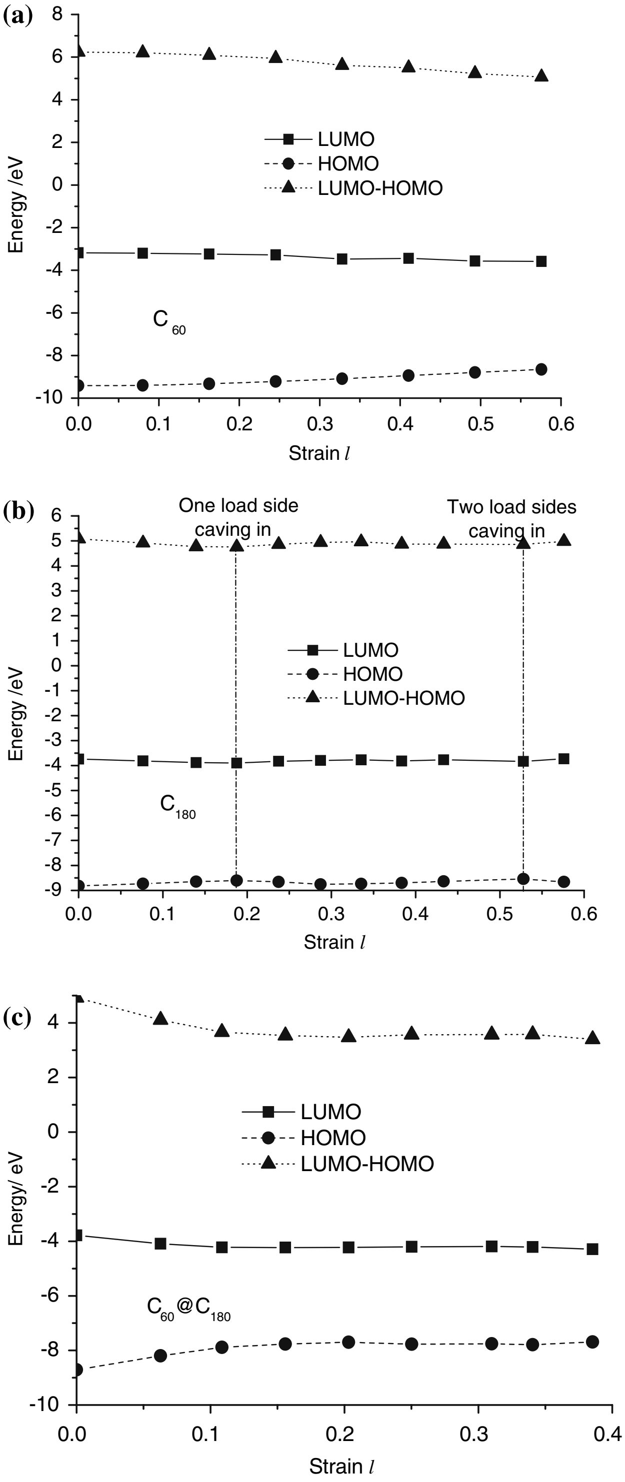

Fig. 7 The LUMO, HOMO energy and their energy-gap of the compressed (**a**) C_{60}, (**b**) C_{180} and (**c**) $C_{60}@C_{180}$ molecules

Conclusions

The MD method and the semi-empirical QM method of PM3 are, respectively, used to investigate the mechanical properties and electronic structure of the C_{60}, C_{180} and $C_{60}@C_{180}$ fullerene molecules under compression. According to the calculated results, the differences of the mechanical properties, as well as the changes of the electronic structure during compression, for three fullerene molecules are discussed. The results show that (1) the C_{60} molecule has the best loading-support and energy-absorbing capability, and the $C_{60}@C_{180}$ molecule has the comparative loading-support and energy-absorbing capability to the C_{180}, (2) of three molecules the $C_{60}@C_{180}$ molecule has the worst chemical-stability and the C_{60} molecule has the best one, and (3) the compressed C_{60} and $C_{60}@C_{180}$ molecules become more chemically active and easier to lose electron, and when the C_{180} molecule caves in at loading-position(s), it suddenly becomes chemically unstable.

Acknowledgement This work is supported by the Innovation Foundation of NUAA (Y0507-013).

References

1. Kroto HW, Heath JR, Brien SC, Curl RF, Smalley RE (1985) Nature 318:162
2. Prinzbach H, Weiler A, Landenberger P, Wahl F, Wörth J, Scott LT, Gelmont M, Olevano D, Issendorff BV (2000) Nature 407:60
3. Piskoti C, Yarger J, Zettl A (1998) Nature 393:771
4. Kroto HW (1987) Nature 329:529
5. Turker L (2003) J Mol Struct (Theochem) 626:203
6. Shen H (2005) J Funct Mater 36:930
7. Turker L (2002) J Mol Struct (Theochem) 619:107
8. Turker L (2002) J Mol Struct (Theochem) 588:127
9. Turker L (2002) J Mol Struct (Theochem) 577:205
10. Turker L (2004) J Mol Struct (Theochem) 674:15
11. Sariciftci NS, Smilowitz L, Heeger AJ, Wud F (1992) Science 258:1474
12. Zhou F, Yau SL, Jehoulet C, Laude DA, Guan Z, Bard AJ (1992) J Phys Chem 96:4160
13. Shen H (2004) J Mater Res 18:647
14. Wang Y, Wang X, Ni X, Wu H (2003) Acta Phys Sin 52:3120
15. Stewart JP (1989) J Comput Chem 10:209
16. Brenner DW (1990) Phys Rev B 42:9458
17. Robertson DH, Brenner DW, White CT (1992) J Phys Chem 96:6133
18. Mowrey RC, Brenner DW, Dunlap BI, Mintmire JW, White CT (1991) J Phys Chem 95:7138
19. Rafizadeh HA (1974) Physica 74:135
20. Brenner DW, Shenderova OA, Harrison J, Stuart SJ (2002) J Phys Condens Matter 14:783
21. Brenner W, Harrison JA, White CT, Colton RJ (1991) Thin Solid Films 206:220
22. Leach AR (1996) Molecular modeling. Addison Wesley Longman Limited, England
23. Nose S (1984) J Chem Phys 81:511
24. Xie J, Pan Z (1998) Nuclear Technol 21:397
25. Li R, Shang Z (2003) Chin J Struct Chem 22:577
26. Yu Q, Zhu L (1998) Introduction into molecular design. Higher Education Press, Beijing, p 67
27. Fleming I (2003) Frontier orbitals and organic chemical reactions. Wiley Publisher, Indianapolis